Boundary condition analysis for Cuk, Sepic and Zeta converters using energy factor concept

Article *in* Journal of Circuits, Systems and Computers · February 2013

DOI: 10.1142/S0218126612500673

CITATIONS
2

READS
983

3 authors, including:

K.W.E. Cheng
The Hong Kong Polytechnic University
420 PUBLICATIONS **5,115** CITATIONS

SEE PROFILE

S.L. Ho
The Hong Kong Polytechnic University
495 PUBLICATIONS **6,242** CITATIONS

SEE PROFILE

Journal of Circuits, Systems, and Computers
Vol. 22, No. 1 (2013) 1250067 (15 pages)

DOI: 10.1142/S0218126612500673

World Scientific
www.worldscientific.com

BOUNDARY CONDITION ANALYSIS FOR CUK, SEPIC AND ZETA CONVERTERS USING ENERGY FACTOR CONCEPT*

ZHANGHAI SHI†, K. W. ERIC CHENG‡ and S. L. HO§

Department of Electrical Engineering,
The Hong Kong Polytechnic University, Hong Kong
†*ee.zhhshi@polyu.edu.hk*
‡*eeecheng@polyu.edu.hk*
§*eeslho@polyu.edu.hk*

Received 19 September 2011
Accepted 30 May 2012
Published 6 February 2013

This paper aims to use the concept of energy factor and its associated concepts to analyze high-order converters, such as Cuk, Sepic and Zeta converters. The maximum variation of energy factor (MVEF) of high-order converters exhibits particular characteristic which is different from that of second order converters. To carry out the analysis based on MVEF, boundary conditions for the high-order converters should be restudied. There are new boundary conditions that are derived by analyzing the energy factor. Through the research in this paper, it can be concluded that the MVEF can reveal the amount of energy storage and impact the efficiency of high-order converters. Experimental results have confirmed that the MVEF and efficiency are correlated. MVEF can be a preferred index for DC-DC converters including high-order converters.

Keywords: Boundary condition; DC-DC converter; energy factor.

1. Introduction

Energy stored in the reactive components of power converters is the basic and necessary method for power conversion. The energy is temporarily stored and delivered to the output stage or other terminals periodically subject to the switching frequency. This inherent property has not been explored thoroughly to power converters, especially the storage energy with aspects to the power throughput under different converter operation parameters.

In terms of DC-DC converters, the ratio of stored energy to throughput energy can reflect the "mass" or "inertia" of converters. This ratio deserves special attention and intensive study. For this reason, the concept of energy factor has been put

*This paper was recommended by Regional Editor Piero Malcovati.
‡Corresponding author.

forward and introduced as stored energy ratio for DC-DC converters in Refs. 1−4. In Ref. 1, the variation of energy storage ratio, which is called maximum storage energy factor (MSEF), has been examined for different DC-DC converters. The relationship of MSEF and efficiency of DC-DC converter has also been identified for Buck, Boost and Buck-Boost converters. Reference 2 uses the similar concept to analysis isolated converters such as Forward, Flyback and isolated Boost converters. Energy storage has a close relationship with the modeling of DC-DC converters. In Refs. 3 and 4, energy factor has been applied to build model, carry out small-signal analysis and design controller for DC-DC converters. As energy plays an important role on system control, lots of nonlinear control methods for DC-DC converters are based on energy.[5,6] The novel optimal controls on switched-capacitor converters using energy are also reported in Refs. 7 and 8.

On the other hand, the variation of storage energy in DC-DC converter can be viewed as a kind of non-active circulating energy. The previous studies[9−12] on reactive power and power factor applied to power electronic systems are only restricted to the power factor correction externally through a cascaded circuit rather than through the circuit and parameter analysis on a DC system. Classical concepts of "reactive power" and "power factor" cannot be applied directly to evaluate the non-active power of DC systems. It is necessary to develop an alternative method to measure the effectiveness of the power being handled by DC systems, especially DC-DC converters. Such efforts have been initiated by previous scholars. Lawrenson *et al.* has proposed a goodness factor for switched reluctance motor (SRM) to express the ratio of active power processed by SRM.[13] Xue *et al.* elaborated the concept of DC power factor and applied such concept in the analyses of SRM.[14−16] In the field of DC-DC switching power converters, energy factor proposed in Refs. 1−4 can be used as the measurement of non-active power. This point has been elaborated in Ref. 17 which summarizes the previous research on energy factor and proposes the concept "buffer energy factor" to measure the non-active power existed in DC-DC converters. In Ref. 17, the correlations and differences between buffer energy factor and power factor have also been discovered.

Previous researches on energy factor are only concentrated in basic second-order converters. This paper aims to utilize energy factor and its accompanying concepts proposed in Refs. 1−4 to analyze the characteristics of storage energy in higher order DC-DC converters which include Cuk, Sepic and Zeta converters. Higher-order DC-DC converters include a number of passive components. They are more complex than second-order converters, especially under discontinuous mode (DCM). The energy factors of higher order converters show different characteristics. They have more than one case under DCM. The division of DCM for higher order converters is revisited in this paper. The implication of energy storage on the overall efficiency is examined.

The structure of this article is as follows. Section 2 reviews the definitions of energy factor and its accompanying concepts. Section 3 presents the methods to

obtain the formulations of energy factor for higher order converters. The boundary conditions of conduction mode are revisited. Section 4 explores the characteristics of energy factor for higher-order converters. The relationships between energy factor and the parameters of converters are clarified. Section 5 presents the experimental results of efficiency against energy factor for different converters. Section 6 concludes the study.

2. Review on the Definitions of Energy Factor

To research the energy behavior of DC-DC converters, the concepts "storage energy" and "energy factor" have been defined by researchers.[1–4] This section reviews and describes the definitions for energy factor and its related concepts for clarification. The important definitions of these concepts are as follows.

E_S: the *energy storage* in passive components. For inductor L, its stored energy at current i is shown in (1); for capacitor C, its stored energy at voltage v is shown in (2).

$$E_{\mathrm{SL}} = Li^2/2\,, \tag{1}$$

$$E_{\mathrm{SC}} = Cv^2/2\,. \tag{2}$$

ΔE_S: the *maximum variation of energy storage* in each cycle at steady state of DC-DC converter.

$$\Delta E_S = E_{S\max} - E_{S\min}\,. \tag{3}$$

F_E: *energy factor*, that is the ratio of the energy storage to the output energy, i.e.,

$$F_E = E_S/(V_o I_o T_S)\,. \tag{4}$$

ΔF_E: the *maximum variation of energy factor* ($MVEF$), i.e.,

$$\Delta F_E = \Delta E_S/(V_o I_o T_S)\,, \tag{5}$$

where V_o, I_o and T_s are the output voltage, output current and period of the switching cycle, respectively, of DC-DC converters system under steady state.

The basic energy equation can be applied to various passive components as follows.

(1) *Inductor*

At steady state the current of inductor varies periodically. The current increases from a minimum to a maximum and then returns to a minimum. Assume the variation is linear, therefore

$$\Delta E_{\mathrm{SL}} = L(I_{L\max}^2 - I_{L\min}^2)/2\,, \tag{6}$$

where $I_{L\max}$ and $I_{L\min}$ are the peak and trough values, respectively. If the current waveform has an average value $\overline{i_L}$, under continuous mode, then ΔE_{SL} can be

reduced to

$$\Delta E_{\mathrm{SL}} = L\overline{i_L}\Delta i_L\,, \tag{7}$$

where Δi_L is the peak-to-peak current ripple of L.

$$F_{\mathrm{EL}} = E_{\mathrm{SL}}/(V_o I_o T_S)\,, \tag{8}$$

$$\Delta F_{\mathrm{EL}} = \Delta E_{\mathrm{SL}}/(V_o I_o T_S)\,. \tag{9}$$

(2) *Capacitor*

Similarly, the variation of stored energy for a capacitor C can be expressed as

$$\Delta E_{\mathrm{SC}} = C(V_{C\max}^2 - V_{C\min}^2)/2\,, \tag{10}$$

where $V_{C\max}$ and $V_{C\min}$ are the peak and trough values of capacitor's voltage, respectively. Under CCM, if the voltage has an average value $\overline{V_C}$, then ΔE_{SC} can be reduced to

$$\Delta E_{\mathrm{SC}} = C\overline{V_C}\Delta V_C\,, \tag{11}$$

where ΔV_C is the peak-to-peak voltage ripple of capacitor.

$$F_{\mathrm{EC}} = E_{\mathrm{SC}}/(V_o I_o T_S)\,, \tag{12}$$

$$\Delta F_{\mathrm{EC}} = \Delta E_{\mathrm{SC}}/(V_o I_o T_S)\,. \tag{13}$$

(3) *Total energy factor and its variation*

The total energy factor and its variation for all the energy-storage components are direct summations.

$$F_E = \sum_{L,C}(F_{\mathrm{EL}} + F_{\mathrm{EC}})\,, \tag{14}$$

$$\Delta F_E = \sum_{L,C}(\Delta F_{\mathrm{EL}} + \Delta F_{\mathrm{EC}})\,. \tag{15}$$

The above equations denote the maximum energy variation with aspect to the output energy in one cycle. F_E and ΔF_E stand for the ratio of energy storage and the maximum variation of energy storage to output energy for a DC system respectively.

3. The Characteristics of Storage Energy in Three Higher-Order Converters

The classical switched-mode power converters have been fully explored for voltage conversion and control analysis, but its energy handling for each component has not been explored thoroughly. This section explores the energy behavior of passive components in Cuk, Sepic and Zeta converters based on the MVEF defined above.

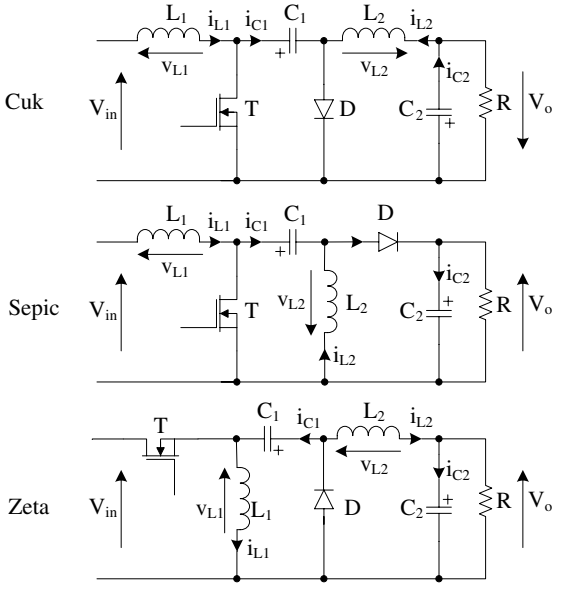

Fig. 1. Three high-order converters.

The topologies of these converters and symbols for components are shown in Fig. 1. The circuits are assumed to operate under ideal condition including negligible loss and linear magnetic and electric characteristics for inductor and capacitor.

3.1. *Cuk converter*

The circuit of Cuk converter and symbols of components are shown in Fig. 1. Figure 2 shows the process from CCM to DCM. It is noted that the Cuk converter under DCM is obviously more complex than the basic second order converters. It has two sub-modes under DCM.

(1) *Continuous mode*

Figure 2(a) shows the typical waveforms of Cuk converter under CCM. The current ripple and average current of inductor L_1 under this mode can be expressed as

$$\Delta i_{L1} = V_{\text{in}} D T_S / L_1 \,, \tag{16}$$

$$\overline{i_{L1}} = I_{\text{in}} \,. \tag{17}$$

Substituting (16) and (17) into (7) and (9), the *variation of energy storage* ΔE_{SL1} and *maximum variation of energy factor* $(MVEF)$ ΔE_{EL1}, as following expressions, can be obtained.

$$\Delta E_{\text{SL1}} = D V_o I_o T_S \,, \tag{18}$$

$$\Delta F_{\text{EL1}} = D \,. \tag{19}$$

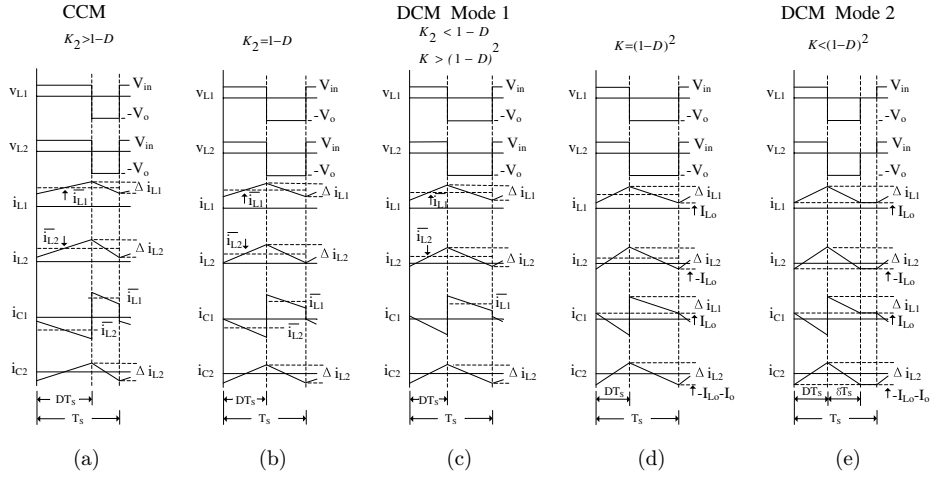

Fig. 2. The operation waveforms of Cuk converter under different modes. K_1, K_2 and $K$are defined as (20).

Table 1 lists the MVEF of components L_2, C_1 and C_2 of Cuk converter under CCM, which can be worked out by the same procedure as that of L_1.

(2) *Discontinuous mode*

The inductor currents of Cuk converter for DCM analysis should be considered for the interaction between the two inductors L_1 and L_2. The analysis is firstly started with the DCM of output inductor, i.e., L_2 (The case for DCM of L_1 is similar and will not be repeated here). Secondly, when the basic second-order converters (Buck, Boost and Buck-Boost) go into DCM, the inductor current will be zero during off time. But when Cuk converter goes into DCM, the inductor current can be reversed. This leads to more than one situation for the DCM of Cuk converter. As Fig. 2 shows, if L_2 works in DCM, then during off time, its current should be zero at first, and then decreases below zero until the diode stops conduction. The waveforms in Fig. 2 show the course to DCM.

There are two situations of DCM of Cuk converter which are shown in Figs. 2(c) and 2(e). The critical points between these situations are: (1) at the end of off time, i_{L2} touches zero; (2) at the end of off time, i_{L2} reverses, but i_D reaches zero. Figures 2(b) and 2(d) show these two critical situations. So there are totally two discontinuous modes for the Cuk converter and their start points are the above two critical situations, which can be determined by the circuit parameters.[18] It is useful to identify the critical conditions by defining these parameters: K_1, K_2 and K as follows.

$$K_1 = 2L_1/(RT_s)\,, \quad K_2 = 2L_2/(RT_s)\,, \quad K = K_1K_2/(K_1+K_2)\,. \tag{20}$$

In (20), L_1, L_2 are inductance of the two inductors of Cuk converter respectively. R is the resistance of load. T_s is the switching period. Such definitions for K_1, K_2 and K

hold true for the analysis of Sepic and Zeta converter. Now parameters about storage energy for the two discontinuous modes of Cuk converter shown in Figs. 2(c) and 2(e) are calculated respectively.

***Mode* 1**

This mode is between critical situations (b) and (d) in Fig. 2. The critical condition from CCM to this mode is

$$\Delta i_{L2} = 2I_o\,. \tag{21}$$

Then by waveform analysis, the critical condition can be simplified as (22)

$$K_2 = 1 - D\,. \tag{22}$$

(a) L_1: As Fig. 2(c) shows, the situation of L_1 is the same as that under CCM. Therefore

$$\Delta F_{\mathrm{EL1}} = D\,. \tag{23}$$

(b) L_2: The maximum variation of storage energy is

$$\Delta E_{\mathrm{SL2}} = L_2 I_{L2\,\max}^2/2\,. \tag{24}$$

Using the same procedure as L_1 and some basic equations of Cuk converter,[18] we can obtain the MVEF of L_2 as (25).

$$\Delta F_{\mathrm{EL2}} = (1 + K_2 - D)^2/(4K_2)\,. \tag{25}$$

(c) C_1: As Fig. 2(c) shows that,

$$\overline{V}_{C1} = V_{\mathrm{in}} + V_o \tag{26}$$

ΔV_{C1} can be calculated by using the area below the horizontal axes of i_{C1}

$$\Delta V_{C1} = \frac{1}{C_1} \cdot \left(\frac{I_o + \frac{1}{2}\Delta i_{L2}}{\Delta i_{L2}} \right)^2 \cdot \frac{1}{2} \cdot DT_S \cdot \Delta i_{L2}\,. \tag{27}$$

Substituting (26) and (27) into (13), one can get

$$\Delta F_{\mathrm{EC1}} = \frac{(K_2 + 1 - D)^2}{4K_2(1 - D)}\,. \tag{28}$$

(d) C_2: As Fig. 2(c) shows, under this mode, the situation of C_2 is the same as that under CCM. So

$$\Delta F_{\mathrm{EC2}} = (1 - D)/(4K_2)\,. \tag{29}$$

***Mode* 2**

This mode emerges after the critical situation (d) occurs in Fig. 2. The critical condition from DCM mode 1 to this mode is

$$K = (1 - D)^2\,. \tag{30}$$

There is a flat part in the waveforms of i_{L1} and i_{L2}. The value I_{Lo} of the flat part can be expressed by the parameters of circuit,[18] here only the results of I_{Lo} and voltage conversion ratio are provided.

$$I_{Lo} = V_{\text{in}} DT_S(D/L_2 - \delta/L_1)/2\,, \tag{31}$$

$$V_o/V_{\text{in}} = D/\delta\,, \tag{32}$$

where $\delta = \sqrt{K}$, $K = 2L_{12}/(RT_S)$, $L_{12} = L_1L_2/(L_1 + L_2)$.

(a) L_1: As Fig. 2(e) shows,

$$\Delta E_{\text{SL1}} = \frac{1}{2} L_1[(I_{Lo} + \Delta i_{L1})^2 - I_{LO}^2]\,. \tag{33}$$

Substitute (31) and (33) into (9), one can get

$$\Delta F_{\text{EL1}} = 1 - \delta + (D + \delta - 1)K/K_2\,. \tag{34}$$

(b) L_2:

$$\Delta E_{\text{SL2}} = \frac{1}{2} L_2(\Delta i_{L2} - I_{Lo})^2\,. \tag{35}$$

Substitute (35) and (31) into (9), then

$$\Delta F_{\text{EL2}} = K_2K(\delta/K + (2 - D - \delta)/K_2)^2/4\,. \tag{36}$$

(c) C_1: Similar to the calculations in Mode 2, $\int_{-ve} i_{C1}dt$ is the area i_{C1} under the horizontal-axis and according to the principle of similar triangles, So

$$\Delta V_{C1} = \frac{1}{C_1} \cdot \left(\frac{\Delta i_{L2} - I_{Lo}}{\Delta i_{L2}}\right)^2 \cdot \frac{1}{2} \cdot DT_S \cdot \Delta i_{L2}\,, \tag{37}$$

$$\overline{V}_{C1} = V_{\text{in}} + V_o\,. \tag{38}$$

Substituting (37) and (38) into (13):

$$\Delta F_{\text{EC1}} = \frac{\delta(D + \delta)}{K_2} \cdot \left(1 - \frac{D + \delta}{2} + \frac{K_2\delta}{2K}\right)^2. \tag{39}$$

(d) C_2:

$$\overline{V}_{C2} = V_o \tag{40}$$

ΔV_{C2} can be calculated by the waveform area of C_2 above the horizontal axis. That is:

$$\Delta V_{C2} = \frac{1}{C_2} \cdot \frac{1}{2}(D + \delta)T_S \cdot \Delta i_{L2} \cdot \left(\frac{\Delta i_{L2} - I_o - I_{Lo}}{\Delta i_{L2}}\right). \tag{41}$$

Substituting (40) and (41) into (13), then

$$\Delta F_{\text{EC2}} = (1 - D/2 - \delta/2)^2(1 + D/\delta)K/K_2\,. \tag{42}$$

Table 1. MVEF of the component of Cuk converter.

Cuk	ΔF_{EL1}	ΔF_{EL2}	ΔF_{EC1}	ΔF_{EC2}
CCM	D	$1-D$	1	$\frac{1-D}{4K_2}$
DCM Mode 1	D	$\frac{(1+K_2-D)^2}{4K_2}$	$\frac{(1+K_2-D)^2}{4K_2(1-D)}$	$\frac{1-D}{4K_2}$
DCM Mode 2	$1-\delta+(D+\delta-1)\frac{K}{K_2}$	$\frac{K_2K}{4}\left(\frac{\delta}{K}+\frac{2-D-\delta}{K_2}\right)^2$	$\frac{\delta(D+\delta)}{K_2}\left(\frac{2-D-\delta}{2}+\frac{K_2\delta}{2K}\right)^2$	$\left(1-\frac{D+\delta}{2}\right)^2\cdot\frac{D+\delta}{\delta}\frac{K}{K_2}$

Results of MVEF of all passive components under different modes are listed in Table 1. Their sum under each mode is the total MVEF for the whole circuit.

3.2. *Sepic and Zeta converter*

Typical Sepic and Zeta converters are also shown in Fig. 1. Their operational waveforms are similar to that of the Cuk converter.[18] The process from CCM to DCM also resembles that of Cuk converter. They also have two modes under DCM.

The MVEF of the passive components of Sepic and Zeta converters can be easily deduced based on the results of Cuk converter. Their expressions under different modes are listed in Tables 2 and 3. The sum of MVEF under each mode is the total MVEF for the whole circuit.

The boundary conditions between different modes of Sepic and Zeta converters are same as those of Cuk converter shown in Fig. 2. Special attention is paid to the

Table 2. MVEF of the component of Sepic converter.

Sepic	ΔF_{EL1}	ΔF_{EL2}	ΔF_{EC1}	ΔF_{EC2}
CCM	D	$1-D$	$1-D$	D or $\frac{(1-D)^2}{4K}\cdot\left[1+\frac{DK}{(1-D)^2}\right]^2$
DCM Mode 1	D	$\frac{(1+K_2-D)^2}{4K_2}$	$\frac{(1+K_2-D)^2}{4K_2}$	
DCM Mode 2	$1-\delta+(D+\delta-1)\frac{K}{K_2}$	$\frac{K_2K}{4}\left(\frac{\delta}{K}+\frac{2-D-\delta}{K_2}\right)^2$	$\frac{\delta^2}{K_2}\left(\frac{2-D-\delta}{2}+\frac{K_2\delta}{2K}\right)^2$	$\frac{(2\delta-K)^2}{4K}$

Table 3. MVEF of the component of Zeta converter.

Zeta	ΔF_{EL1}	ΔF_{EL2}	ΔF_{EC1}	ΔF_{EC2}
CCM	D	$1-D$	$1-D$	$\frac{1-D}{4K_2}$
DCM Mode 1	D	$\frac{(1+K_2-D)^2}{4K_2}$	$\frac{D(1+K_2-D)^2}{4K_2(1-D)}$	$\frac{1-D}{4K_2}$
DCM Mode 2	$1-\delta+(D+\delta-1)\frac{K}{K_2}$	$\frac{K_2K}{4}\left(\frac{\delta}{K}+\frac{2-D-\delta}{K_2}\right)^2$	$\frac{\delta D}{K_2}\left(\frac{2-D-\delta}{2}+\frac{K_2\delta}{2K}\right)^2$	$\left(1-\frac{D+\delta}{2}\right)^2\cdot\frac{D+\delta}{\delta}\frac{K}{K_2}$

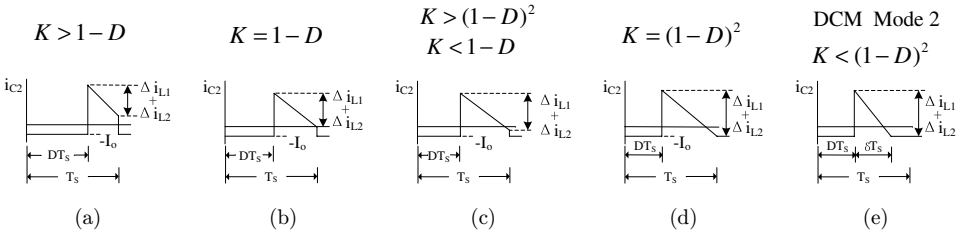

Fig. 3. The operation waveforms of capacitor C_2 in Sepic under different modes. K_1, K_2 and K are defined as (20).

voltage waveform of C_2 in Sepic. It is different from that in Cuk and Zeta converters. This will cause the boundary conditions between states of C_2 in Sepic are different from those in Cuk and Zeta converters. The operation of C_2 in Sepic still has three modes as illustrated by Fig. 3. In the five states in Figs. 3(b) and 3(d) are boundary states. State (e) corresponds to the DCM Mode 2. But states (a) and (c) can be taken place at any moment during CCM and DCM Mode 1. It depends on the value of K and D. In fact, based on Fig. 3, the boundary condition for state (b), which is the transition from (a) to (c), can be calculated as follows:

$$\bar{i}_{L1} - \frac{1}{2}\Delta i_{L1} + \bar{i}_{L2} - \frac{1}{2}\Delta i_{L2} - I_o = 0\,. \tag{43}$$

Simplifying (43), the boundary condition for the transitional state (b) is:

$$K = 1 - D\,. \tag{44}$$

It can be seen that this boundary condition is different from $K_2 = 1 - D$, which is the boundary condition from CCM to DCM Mode 1 in Cuk and Zeta converter.

The MVEF of C_2 in Sepic can be deduced by (13) like the MVEF of other reactive components. Its results are listed in Table 2.

4. Consolidation of the Energy Factor

Figures 4–6 show the MVEF of Cuk, Sepic and Zeta converters as a function of duty ratio D. For simplicity, $K = K_2$ are assumed. This assumption is justified when K_2 is much smaller than K_1. K_1, K_2 and K are defined as (20). It is also noted that L_1 works under CCM.

All three converters have continuity characteristics between different operation modes. The boundary conditions between different operation modes are the same for all three converters. Figures 4–6 also illuminate the continuity of the curves.

As mentioned before, the sum of each component's MVEF is the MVEF of whole converter. Figure 4 shows the characteristics of MVEF of the Cuk converter. It can be seen that for Cuk converter, MVEF is always larger than 2. It decreases as K increases. For $K \geq 1$, the relationship between MVEF and D is linear. MVEF

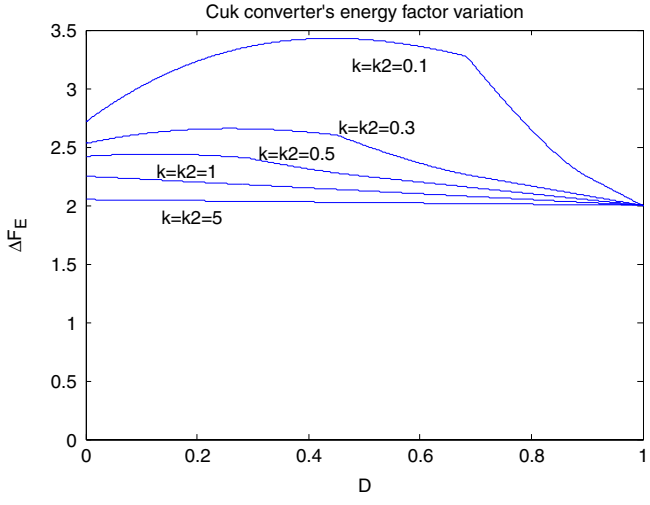

Fig. 4. MVEF of the Cuk convertor (color online).

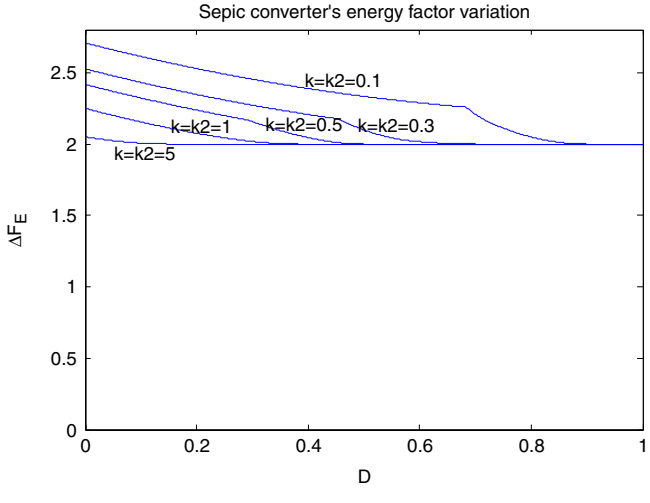

Fig. 5. MVEF of the Sepic convertor (color online).

decreases as D increases. For $K < 1$, the characteristic exhibits a portion of nonlinearity because of the discontinuous inductor conduction mode. The lower limit of MVEF is 2 and is independent of K. The lower limit of MVEF can be reached when the transistor is always turned on.

Figure 5 shows MVEF characteristics for Sepic. It can be seen that MVEF of Sepic is always no less than 2. It decreases as K and D increase. For $K \geq 1$, a large portion of MVEF maintains the value of 2. For $K < 1$, the characteristic exhibits a

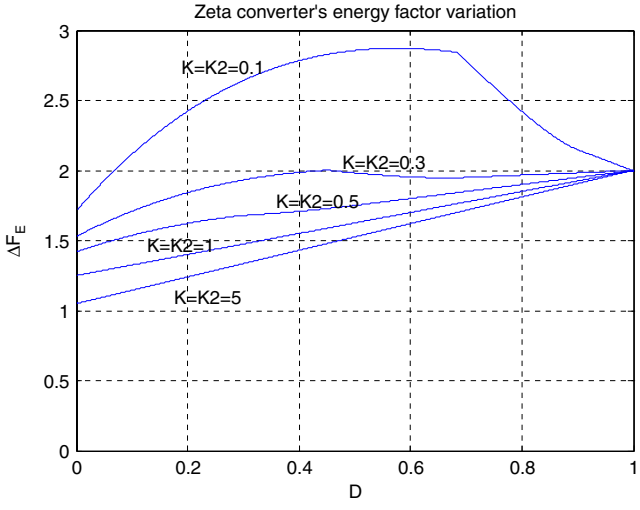

Fig. 6. MVEF of the Zeta convertor (color online).

portion of nonlinearity again because of the discontinuous mode. MVEF reaches the maximum value when the transistor is always turned on.

The MVEF characteristic for Zeta converter is shown in Fig. 6, which is different from that of the Cuk converter. MVEF of Zeta also decreases when K increases. MVEF varies linearly with D when $K \geq 1$. It reaches maximum value of 2 at $D = 1$. For $K < 1$, the nonlinear portion of the curve is again due to discontinuous mode. And the maximum value of MVEF does not occur at $D = 1$, but occurs when D is at certain value between 0 and 1.

In general, for all the three converters, MVEF increases as K decreases. This is the universal property shared by the three basic second order converters (Buck, Boost and Buck-Boost converter).[1]

The MVEF can also indicate the amount of non-active energy circulating inside the converters which will cause power loss and the loss of voltage conversion ratio. Figure 7 compares the MVEF of the Cuk, SEPIC and Zeta converters under CCM. The simulation parameters are $R = 10\,\Omega$, $L_1 = L_2 = 100\,\mu$H, $C_1 = C_2 = 100\,\mu$F and $f_s = 100\,$kHz. From Fig. 7, it is found that the Cuk converter has the highest amount of non-active circulating energy whereas the Zeta converter has the least amount. This indicates that the Zeta converter has the best inner energy characteristic although its input current is discontinuous all the time.

5. Experimental Results

Figure 7 shows the experimental results of efficiency against MVEF for Cuk and Zeta converters. The circuits for experiments are the same as Fig. 1, $L_1 = L_2 = 340\,\mu$H,

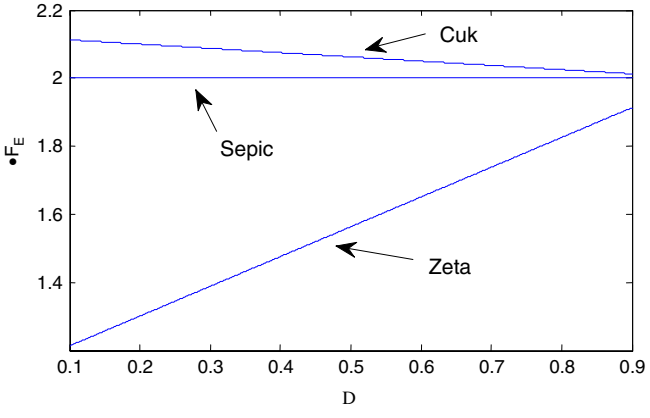

Fig. 7. Comparison of MVEF among Cuk, Sepic and Zeta converters (color online).

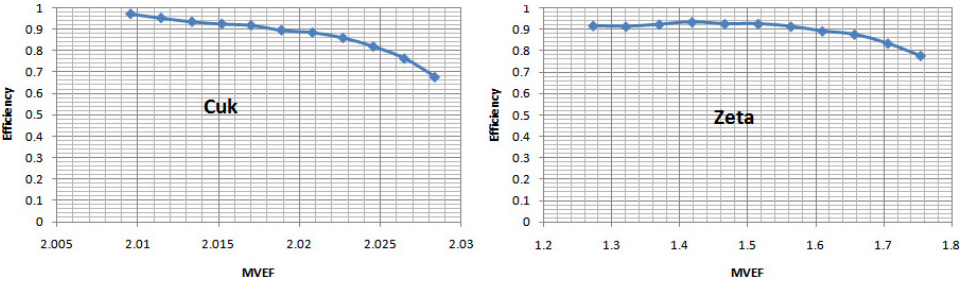

Fig. 8. Efficiency against MVEF for Cuk and Zeta converter (color online).

$C_1 = C_2 = 220\,\mu$F, $f_s = 100\,$kHz, the load is set as $R = 10.07\,\Omega$, output voltage is set as $V_o = 30\,$V and output power is set as 90 W. Then the circuit parameters $K_1 = K_2 = 6.8$, $K = 3.4$ are determined for the test. Low $R_{\mathrm{ds(on)}}$ MOSFET IRFB4227PBF is used. The converters work under the continuous mode. Duty ratio is varied to give different MVEFs for the experiments. The MVEF covers 2.0096−2.0284 for the Cuk converter and 1.272−1.754 for the Zeta converter. Beyond this range it will be very difficult to operate due to either a very large voltage or current in the circuits. Figure 8 shows that the efficiency decreases as MVEF increases for most values of MVEF as expected.

For Sepic converter, MVEF is 2 for continuous mode. Its efficiency versus MVEF is simple and its experimental results is not conducted in this test.

6. Conclusion

The concept of energy factor and its associated concepts proposed by previous scholars can be used to analysis high-order converters. The MVEF of high-order

converters exhibits particular characteristics which is different from that of second-order converters. This is caused by the complexity of high-order converters which contain more passive components. To carry out the analysis based on energy factor, boundary conditions for the high-order converters should be restudied. There are new boundaries seen through the exercise of energy factor. The new boundaries are clarified in the paper. The MVEF for Cuk, Sepic and Zeta converter are analyzed under three modes. It is expected that the efficiency of converters decreased as MVEF increases. Experimental results for Cuk and Zeta converters confirm the relationship between energy factor and efficiency.

Through the research in this paper, it can be concluded that MVEF is a preferred index for DC-DC converters including high-order converters. MVEF can reveal the amount of energy storage in DC-DC converters. MVEF also has impact on the efficiency of DC-DC converters. When MVEF is small, that means the inductor/capacitor only deals with small amount of energy variation, the size of inductor and capacitor may be smaller. This also indicates that the power loss will be relatively low and the efficiency is expected to be high.

Acknowledgment

The authors gratefully acknowledge the financial support of the Research Grants Council (RGC) of Hong Kong (PolyU5136/06E) and The Hong Kong Polytechnic University (B-Q02W) for this project.

References

1. K. W. E. Cheng, Storage energy for classical switched mode power converters, *IEE Proc.-Electr. Power Appl.* **150** (2003) 439−446.
2. K. W. E. Cheng and Y. Lu, Formulation of the energy-storage factor for isolated power convertors using integrated magnetics, *IEE Proc.-Electr. Power Appl.* **152** (2005) 837−844.
3. F. L. Luo and H. Ye, Energy factor and mathematical modelling for power DC/DC converters, *IEE Proc.-Electr. Power Appl.* **152** (2005) 191−198.
4. F. L. Luo and H. Ye, Small signal analysis of energy factor and mathematical modeling for power dc-dc converters, *IEEE Trans. Power Electron.* **22** (2007) 69−79.
5. D. del Puerto-Flores, R. Ortega and J. M. A. Scherpen, A cyclodissipativity characterization of power factor compensation of nonlinear loads under nonsinusoidal conditions, *Int. J. Circuit Theor. Appl.* (2011), DOI: 10.1002.
6. M. Zhu and F. L. Luo, Transient analysis of multi-state dc−dc converters using system energy characteristics, *Int. J. Circuit Theor. Appl.* **36** (2008) 327−344.
7. R. C. Loxton, K. L. Teo, V. Rehbock and W. K. Ling, Optimal switching instants for a switched-capacitor DC/DC power converter, *Automatica* **45** (2009) 973−980.
8. C. Y. F. Ho, B. W. K. Ling, Y. Q. Liu, P. K. S. Tam and K. L. Teo, Optimal PWM control of switched-capacitor DC−DC power converters via model transformation and enhancing control techniques, *IEEE Trans. Circuits Syst. I* **55** (2008) 1382−1391.

9. M. G. Umamaheswari, G. Uma and S. Redline Vijitha, Comparison of hysteresis control and reduced order linear quadratic regulator control for power factor correction using DC-DC Cuk converters, *J. Circuits, Syst., Comput.* **21** (2012), DOI: 10.1142/S0218126612500028.
10. A. I. Maswood and F. Liu, A novel unity power factor input stage for AC drive application, *IEEE Trans. Power Electron.* **20** (2005) 857−863.
11. H. F. Bilgin, K. N. Kose, G. Zenginobuz, M. Ermis, E. N. I. Cadirci and H. Kose, A unity-power-factor buck-type PWM rectifier for medium/high-power DC motor drive applications, *IEEE Trans. Ind. Appl.* **38** (2002) 1412−1425.
12. J. Itoh and K. Fujita, Novel unity power factor circuits using zero-vector control for single-phase input systems, *IEEE Trans. Power Electron.* **15** (2000) 36−43.
13. P. J. Lawrenson, J. M. Stephenson, P. T. Blenkinsop, J. Corda and N. N. Fulton, Variable-speed switched reluctance motors, *IEE Proc., Part B: Electr. Power Appl.* **127** (1980) 253−265.
14. X. D. Xue, K. W. E. Cheng and S. L. Ho, Correlation of modeling techniques and power factor for switched-reluctance machines drives, *IEE Proc.-Electr. Power Appl.* **152**(3) (2005) 710−722.
15. X. D. Xue, K. W. E. Cheng and S. L. Ho, Influences of output and control parameters on power factor of switched reluctance motor drive systems, *Electric Power Compon. Syst.* **32** (2004) 1207−1223.
16. X. D. Xue, K. W. E. Cheng and S. L. Ho, Improvement of power factor in switched reluctance motor drives through optimizing in switching angles, *Electric Power Compon. Syst.* **32** (2004) 1225−1238.
17. Z. Shi, K. W. Eric Cheng and S. L. Ho, Formulation and experimental results of buffer energy and energy factor of DC-DC converters, *Int. J. Circuit Theor. Appl.*, DOI: 10.1002/cta.815. 2011.
18. K. W. E. Cheng, *Classical Switched Mode and Resonant Power Converters* (The Hong Kong Polytechnic University, Hong Kong, 2002).